JACS JOURNAL OF THE AMERICAN CHEMICAL SOCIETY

Communication

Cite This: J. Am. Chem. Soc. 2019, 141, 15003−15007

pubs.acs.org/JACS

Side-On Coordination of Nitrous Oxide to a Mononuclear Cobalt Center

Charles C. Mokhtarzadeh, Chinglin Chan, Curtis E. Moore, Arnold L. Rheingold, and Joshua S. Figueroa*

Department of Chemistry and Biochemistry, University of California, San Diego, 9500 Gilman Drive, Mail Code 0358, La Jolla, California 92093-0358, United States

Supporting Information

ABSTRACT: Despite its utility as an oxygen-atom transfer reagent for transition metals, nitrous oxide (N_2O) is a notoriously poor ligand, and its coordination chemistry has been limited to a few terminal, end-on κ^1-*N* complexes. Here, the synthesis of a mononuclear cobalt complex possessing a side-on-bound N_2O molecule is reported. Structural characterization, IR spectroscopy, and DFT calculations support an η^2-*N,N* binding mode for binding of N_2O to the cobalt center.

Nitrous oxide (N_2O) is now recognized as the third most abundant greenhouse gas (~300 ppb) behind CO_2 (~400 ppm) and CH_4 (~1800 ppb) as a result of increased production from anthropogenic sources.[1−3] The increases in atmospheric N_2O have proven difficult for the global nitrification and denitrification mechanisms to balance,[1,4] which has resulted in deleterious effects on atmospheric ozone concentrations.[5,6] Accordingly, nitrous oxide capture, activation, and use as a potentially "green" oxidant with inorganic and organometallic systems are still prominent areas of study. However, despite the attractiveness of N_2O as an oxidant, its utility in practice is hampered by its high kinetic stability. Break-down of N_2O into its constituents, N_2 and O_2, is not operable in the absence of catalysts until elevated temperatures (~400 °C) owing to a high activation barrier (ca. 59 kcal/mol).[7] Nevertheless, it has been well documented that N_2O can serve as a highly effective oxygen-atom transfer reagent in the presence of many transition-metal-based systems.[8−10] Transition-metal-mediated activation of N_2O generally proceeds via extrusion of dinitrogen, concomitant with the formation of a reactive metal−oxo species, which ultimately facilitates substrate oxidation. In addition, N_2O functionalization by direct insertion into M−C or M−H bonds has been observed.[11−17]

Despite the use of nitrous oxide as an oxidant or oxygen-atom transfer reagent, its activation by transition metals is challenging. It has been well established that N_2O is an exceedingly poor ligand on account of a low dipole moment (0.161 D) and weak σ-donor and π-acceptor abilities.[9,18,19] Accordingly, the coordination chemistry of N_2O is significantly limited. In 1969, Armor and Taube reported the cation $[Ru(NH_3)_5(N_2O)]^+$, which was the first coordination complex featuring a bound N_2O molecule.[20] The thermal instability of $[Ru(NH_3)_5(N_2O)]^+$ precluded its isolation in the solid state. However, spectroscopic and computational studies have provided strong evidence for a terminal, κ^1-*N* coordination mode of the N_2O ligand.[21,22] Since this initial report, only three other discrete examples of transition-metal nitrous oxide complexes have appeared, all of which have been spectroscopically or structurally characterized as terminal κ^1-*N*-N_2O adducts bound to a mononuclear metal center.[23−25] Other coordination modes for N_2O, such as side-on η^2-*N,N*, η^2-*N,O*, and various dinuclear bridging modes, have been considered computationally[9] but have not been authenticated experimentally for coordination complexes. Notably, however, the structure of substrate-loaded N_2O reductase (N_2OR) from *Pseudomonas stutzeri* exhibited a long, side-on interaction of N_2O bridging three Cu centers of a [4Cu:2S] active site.[26] While it has been argued that this structure is not relevant to the mechanism of [4Cu:2S] N_2ORs,[27] this work suggested that side-on binding of N_2O to low-valent metal centers is a potential alternative to terminal, κ^1-*N* coordination.

Our group has shown that sterically encumbering *m*-terphenyl isocyanides can stabilize reactive transition metal centers for use in unusual small-molecule activation processes.[28−31] Here we report the isocyanide-stabilized cobalt complex, $Cp^*Co(N_2)(CNAr^{Tripp2})$ (**1**; Ar^{Tripp2} = 2,6-(2,4,6-(*i*-Pr)$_3C_6H_2)_2C_6H_3$), as a scaffold for the generation of a side-on-bound nitrous oxide complex. In addition to structural determination, we present spectroscopic and computational evidence for an η^2-*N,N* coordination mode for the N_2O ligand. For this mononuclear system, η^2-*N,N* coordination is enabled by the strongly π-basic properties of the low-valent cobalt center within the $Cp^*Co(CNAr^{Tripp2})$ fragment. This electronic match between a side-on coordinated N_2O ligand and a low-valent transition metal affords an adduct that is both activated and persistent in solution in the absence of an N_2O atmosphere. This solution-phase persistence has allowed for a determination of the fragmentation pathways available to side-on-bound N_2O within this system.

Treatment of a toluene-d_8 solution of $Cp^*Co(N_2)(CNAr^{Tripp2})$ (**1**) with an excess of N_2O at −78 °C, followed by rapid injection into a precooled NMR spectrometer, indicated conversion to a new diamagnetic product over the course of 1 h as assayed by ^1H NMR spectroscopy (Figure S3.1). Upon warming, this new species persisted to −25 °C, where it began to rapidly decompose. Accordingly, this

Received: July 31, 2019
Published: September 6, 2019

DOI: 10.1021/jacs.9b08241
J. Am. Chem. Soc. 2019, 141, 15003−15007

experiment was repeated on a preparative scale by treatment of **1** with N_2O in Et_2O solution at −78 °C, followed by cold workup and crystallization at −40 °C under a dinitrogen atmosphere. This procedure afforded yellow/orange single crystals, crystallographic characterization of which determined the product to be the side-on-bound nitrous oxide complex, $Cp^*Co(\eta^2\text{-}N_2O)(CNAr^{Tripp2})$ (**2**; Scheme 1, Figure 1, left).

Scheme 1. Synthetic Route to Complexes 2 and 3

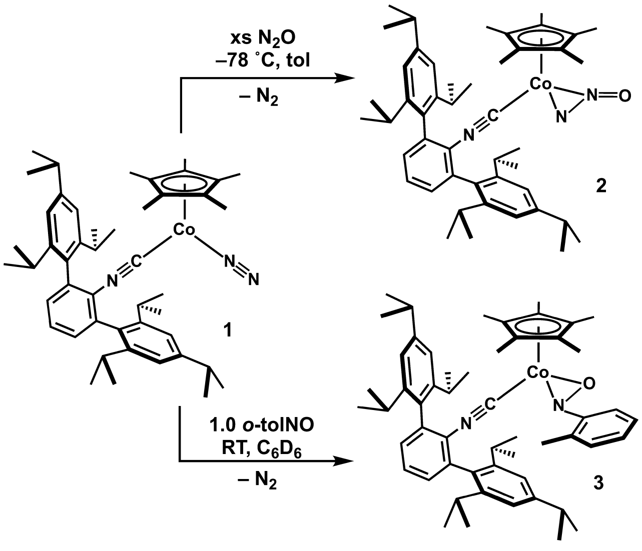

The solid-state structure of complex **2** possesses a 65:35 two-fold positional disorder of the η^2-bound N_2O ligand across the pseudo mirror plane of the $Cp^*Co(CNAr^{Tripp2})$ fragment. While this disorder, and crystallographic structure determination in general, cannot unambiguously differentiate between the coordination of N vs O atoms, the observed structure of **2** in comparison to DFT calculations and the metrical parameters of synthetic model complexes strongly indicate an η^2-*N,N*, rather than η^2-*O,N*, coordination mode. For example, DFT calculations (B3LYP/def2-TZVP) on both the η^2-*N,N*, and η^2-*O,N* isomers of the computational model $Cp^*Co(\eta^2\text{-}N_2O)(CNXyl)$ (**2m**-E_1,E_2; E_1 = N or O, E_2 = N; Xyl = 2,6-$Me_2C_6H_3$) reveal that the η^2-*N,N* isomer is favored over the η^2-*O,N* isomer by 10.3 kcal/mol. In addition, the metrical parameters of the η^2-N_2O unit associated with **2m**-*N,N* are consistent with the experimental structure of complex **2**, whereas those of **2m**-*O,N* vary significantly (Table 1). This is best illustrated by the E_1−E_2 bond distance of the two well-ordered Co-coordinated atoms in **2** (1.212(8) Å), which matches well with that of **2m**-*N,N* (1.199 Å). In contrast, **2m**-*O,N* was calculated to possess a significantly longer η^2-E_1,E_2 bond distance of 1.358 Å.

To provide an independent comparison, the η^2-*N,O* nitrosoarene complex, $Cp^*Co(\eta^2\text{-}O,N\text{-}(o\text{-tolNO}))(CNAr^{Tripp2})$ (**3**; *o*-tolNO = 2-$MeC_6H_4(N{=}O)$), was prepared via treatment of **1** with *ortho*-nitrosotoluene and structurally characterized (Scheme 1, Figure 1).[32] The η^2-*O,N* unit of complex **3** displays a bond distance of 1.371(4) Å, which matches the calculated value for **2m**-*O,N*, but differs significantly from the η^2-E_1,E_2 distance of the N_2O unit in **2**. Accordingly, these comparative metrical and computational data suggest that complex **2** features an η^2-*N,N*-bound N_2O ligand.

In addition to the structural data for complex **2**, solution-phase IR spectroscopy, ^{15}N isotopic labeling studies, and vibrational frequency calculations are also consistent with η^2-*N,N* coordination of the N_2O ligand. Uncalibrated vibrational frequency calculations on **2m**-*N,N* revealed two bands associated with an η^2-*N,N*-bound N_2O ligand at 1757 and 1182 cm^{-1}, which are assigned to ν_{NN} and composite ν_{NNO} stretches, respectively (Figure 2, top). The corresponding calculations for **2m**-*O,N* revealed a single high-energy band at 1902 cm^{-1} assignable to a ν_{NN} stretch, which is consistent with the short N−N bond distance computed for this isomer (Table 1). Furthermore, the calculations for **2m**-*O,N* did not reveal a distinct ν_{NO} band in the region between 2000 and 1000 cm^{-1}, presumably due to the significant elongation of this bond in a putative η^2-*O,N* N_2O complex.

As shown in Figure 2, the low-temperature (−40 °C) FTIR spectrum of ^{14}N-labeled **2** acquired in the presence of free $^{14}N_2O$ gave rise to two low-intensity bands at 1624 and 1131 cm^{-1} assignable to the η^2-*N,N* isomer. These bands are considerably lower in energy than that of free $^{14}N_2O$ (ν_{NNO} = 2223 cm^{-1})[24] and shift to 1573 and 1113 cm^{-1} when complex **2** is generated using $^{15}N_2O$ (Figure 2). Most importantly, the

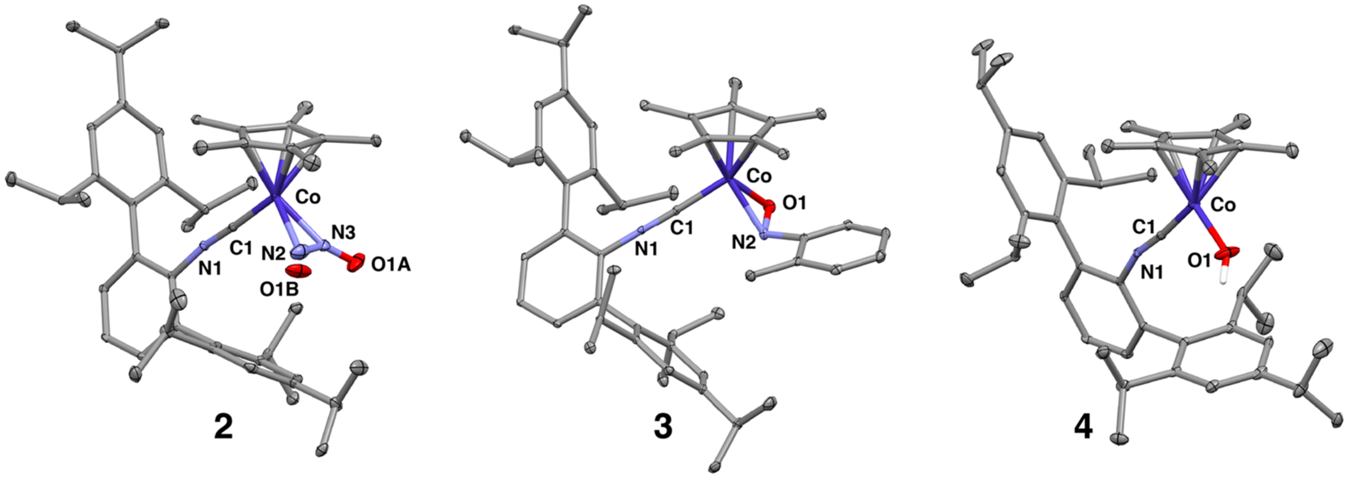

Figure 1. Molecular structures of complexes **2**−**4**. For complex **2**, the minor disorder component is shown as a nonbonded displacement relative to the major component (N2−N3−O1A).

Table 1. Comparison of Experimental and Calculated Metrical Parameters for 2 and the Model Complexes 2m-*N,N* and 2m-*O,N*

	complex **2**	**2m**-*N,N* (calc)	**2m**-*O,N* (calc)
$d(\text{Co}-\text{E}_1)$ (Å)	1.904(5) (Co−N2)	1.983 (Co−N)	1.950 (Co−O)
$d(\text{Co}-\text{E}_2)$ (Å)	1.952(5) (Co−N3)	1.890 (Co−N)	1.897 (Co−N)
$d(\text{E}_1-\text{E}_2)$ (Å)	1.212(8) (N2−N3)	1.199 (N−N)	1.358 (O−N)
$d(\text{E}_2-\text{E}_3)$ (Å)	1.12(1) (N2−O1B), 1.26(1) (N3−O1A)	1.235 (N−O)	1.155 (N−N)
$\angle(\text{E}_1-\text{E}_2-\text{E}_3)$ (deg)	135.2(6) (O1A−N2−N3), 146.5(8) (O1B−N3−N2)	142.6	139.2

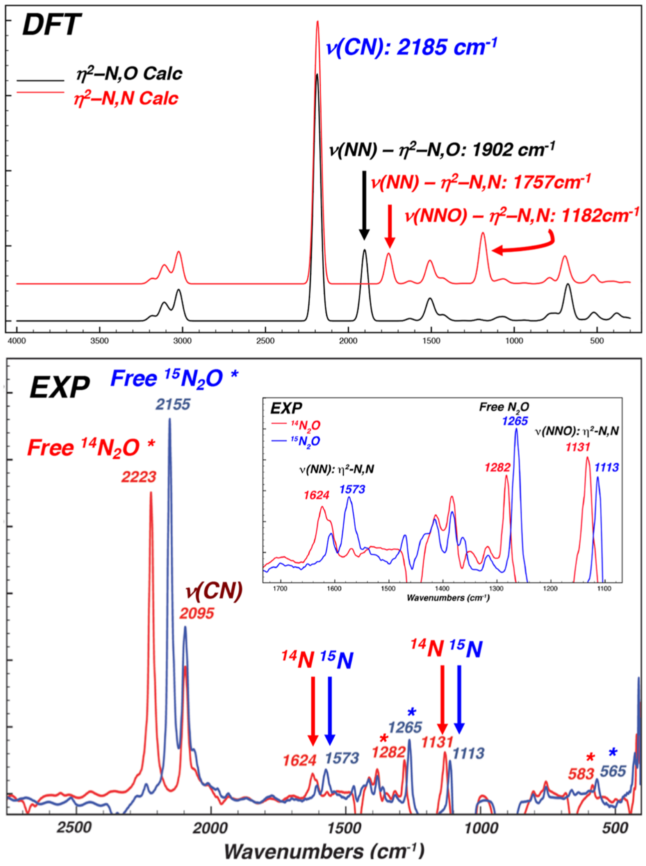

Figure 2. (Top) Calculated ^{14}N IR spectra for models **2m**-*N,N* and **2m**-*O,N*. (Bottom) Overlaid experimental FTIR spectra for ^{14}N-**2** and^{15}N-**2**, with inset showing the region between 1725 and 1075 cm^{-1}.

spectra of ^{14}N-**2** and ^{15}N-**2** do not show a higher-energy (2000−1700 cm^{-1}) N_2O-associated band indicative of an η^2-*O,N* isomer. In addition, it is notable that treatment of the ^{14}N-labeled terminal dinitrogen complex **1** with $^{15}N_2O$ exclusively affords ^{15}N-labeled ^{15}N-**2**. This signifies that intermolecular O-atom transfer between free N_2O and cobalt-coordinated N_2 is not a mechanistic pathway to the formation of complex **2**. Analysis of ^{15}N-**2** by ^{15}N NMR spectroscopy (−40 °C) revealed two doublets at δ = +309 ppm and +159 ppm (J_{NN} = 17 Hz), assigned to the O-^{15}*N*, and ^{15}N-^{15}*N* atoms, respectively. These resonances and coupling constant are significantly different than those found for free N_2O (δ(O-*N*) = +218 ppm, δ(N-*N*) = +135 ppm; J_{NN} = 8.5 Hz)[33] and reflect a distinct perturbation of N_2O upon side-on coordination.[34]

The preference for η^2-*N,N* coordination in **2** can be rationalized on the basis of the electronic characteristics of both the cobalt coordination environment in **2** and the π^* system of N_2O. The Cp*Co(CNAr$^{\text{Tripp}}$) fragment is a derivative of the generic CpCo(L) coordination platform (L = CO, PR_3), which has been used extensively for π-coordination of olefins, alkynes, and other unsaturated substrates.[35−40] This utility of CpCo(L) is derived from the strong π-basic character of the d^8 cobalt center in the plane parallel to the cyclopentadienyl ring. Whereas the π^* system of N_2O possesses greater nitrogen than oxygen character,[9] η^2-*N,N* coordination additionally allows for the accumulation of electron density on the more electronegative oxygen atom (Scheme 2). Such resonance contributions likely serve to stabilize a strong backbonding interaction to the π^* manifold of a side-on-coordinated N_2O molecule. This electronic structure description of complex **2** is reflected in the computed Mulliken charges for the oxygen atom in **2m**-*N,N* relative to that in free N_2O (−0.412 au vs −0.305 au, respectively). In addition, the significantly bent η^2-*N,N*-N_2O ligand found in **2** reflects a disruption of the N_2O π^* system in line with the Dewar−Chatt−Duncanson model for π-backdonation.

Scheme 2. Resonance Contributions for η^2-*N,N* Binding for Complex 2

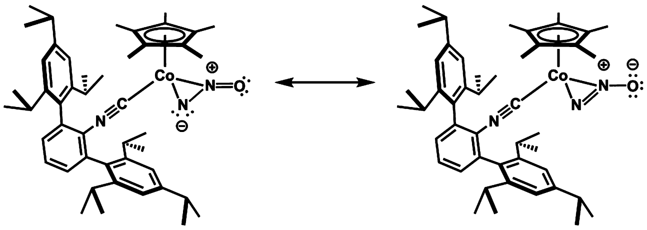

Consistent with the presence of a strong π-backbonding interaction, complex **2** persists in solution in the absence of an N_2O atmosphere, which contrasts with the behavior of some linear κ^1-*N* N_2O adducts.[23,24] *In situ* FTIR experiments conducted at −40 °C in THF revealed that the N_2O atmosphere used to generate complex **2** could be removed by sparging with argon or N_2 (Figure S2.5). No change to the isocyanide ν_{CN} spectroscopic signature for **2** was observed over the course of 2 h after introduction of these gases, and it is notable that the presence of dinitrogen does not return the terminal-N_2 complex **1** (ν_{CN} = 2004 cm^{-1}). Complex **2** can also be subjected briefly to vacuum (∼30 s), resulting in only minimal liberation of N_2O (Figure S2.5).

The decomposition of complex **2** above 0 °C was also investigated and provided insights into the fragmentation of the η^2-bound N_2O ligand. Warming THF or Et_2O solutions of **2** to room temperature, followed by FTIR spectroscopy analysis, indicated the isocyanate, OCNAr$^{\text{Tripp2}}$, as the major product of decomposition. However, ν_{CN} and ν_{OH} bands

DOI: 10.1021/jacs.9b08241
J. Am. Chem. Soc. 2019, 141, 15003−15007

Scheme 3. (Top) Product Distribution for the Decomposition of Complex 2 above −25 °C; (Bottom) Reaction Outcomes between Complex 2 and Triphenylphosphine and Cyclohexene

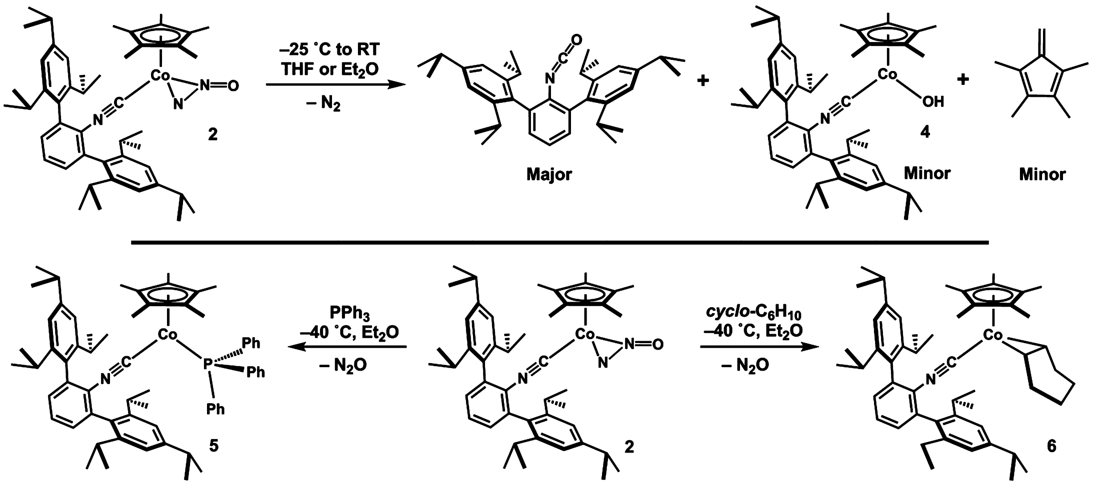

associated with the paramagnetic, terminal hydroxide complex Cp*Co(OH)(CNAr^{Tripp2}) (**4**), which was prepared independently, are also apparent (Scheme 3, Figure 1). Allowing the decomposition of **2** to proceed in THF-d_8 also resulted in ν_{OH}, rather than ν_{OD}, bands for complex **4**, while analysis of the decomposition mixture by ^{1}H NMR spectroscopy revealed the formation of tetramethylfulvalene (Scheme 3).[41] Accordingly, the generation of these products potentially suggests that the decomposition of **2** leads to the formation of a reactive metal−oxygen species capable of intramolecular H-atom abstraction. However, the formation of OCNAr^{Tripp2} also suggests that O-atom transfer to the ancillary isocyanide ligand is highly competitive and may proceed by an independent pathway. Monitoring the decomposition of ^{15}N-**2** by ^{15}N NMR spectroscopy revealed the decay of signals associated with the η^2-*N,N*-bound N_2O ligand concomitant with the appearance of free dinitrogen (δ ^{15}N = +295 ppm),[34] thereby indicating an overall process consistent with O−N bond cleavage. Importantly, treatment of −40 °C Et_2O solutions of complex **2** with either PPh_3 or cyclohexene proceeded exclusively with N_2O loss to Cp*Co(PPh$_3$)(CNAr^{Tripp2}) (**5**) and Cp*Co(η^2-*C,C*-(*cyclo*-C_6H_{10})(CNAr^{Tripp2}) (**6**), respectively (Scheme 3). These reactions indicate that nucleophilic substrates may not induce O-atom transfer from **2**, which is a reactivity profile consistent with the accumulation of electron density on the terminal oxygen atom of an η^2-*N,N*-bound N_2O ligand.

The results presented here demonstrate that N_2O can bind to a mononuclear metal center in a side-on, η^2-*N,N* manner. Given that N_2O has been established to bind in a κ^1-*N* fashion, yet can effectively transfer an oxygen atom to mononuclear metal centers, this side-on binding mode potentially serves as a snapshot of an intramolecular process ultimately leading to O−N bond cleavage.

■ ASSOCIATED CONTENT

Ⓢ Supporting Information

The Supporting Information is available free of charge on the ACS Publications website at DOI: 10.1021/jacs.9b08241.

Synthetic procedures, characterization, and spectroscopic data (PDF)

Crystallographic data (CIF)

■ AUTHOR INFORMATION

Corresponding Author

*jsfig@ucsd.edu

ORCID

Curtis E. Moore: 0000-0002-3311-7155
Joshua S. Figueroa: 0000-0003-2099-5984

Notes

The authors declare no competing financial interest.

■ ACKNOWLEDGMENTS

We are grateful to the U.S. National Science Foundation for support of this work (CHE-1802646) and for a Graduate Research Fellowship to C.C.M. We also thank the Taiwan Ministry of Education for a Graduate Fellowship to C.C.

■ REFERENCES

(1) Kanter, D.; Mauzerall, D. L.; Ravishankara, A. R.; Daniel, J. S.; Portmann, R. W.; Grabiel, P. M.; Moomaw, W. R.; Galloway, J. N. A post-Kyoto partner: Considering the Stratospheric Ozone Regime as a Tool to Manage Nitrous Oxide. *Proc. Natl. Acad. Sci. U. S. A.* **2013**, *110*, 4451−4457.

(2) Kramlich, J. C.; Linak, W. P. Nitrous Oxide Behavior in the Atmosphere, and in Combustion and Industrial Systems. *Prog. Energy Combust. Sci.* **1994**, *20*, 149−202.

(3) Blasing, T. J. *Recent Greenhouse Gas Concentrations*; Carbon Dioxide Information and Analysis Center, Oak Ridge National Laboratory: Oak Ridge, TN, 2016. DOI: 10.3334/CDIAC/atg.032. Accessed July 24, 2019.

(4) Wüst, A.; Schneider, L.; Pomowski, A.; Zumft, W. G.; Kroneck, P. M.; Einsle, O. Nature's Way of Handling a Greenhouse Gas: The Copper-Sulfur Cluster of Purple Nitrous Oxide Reductase. *Biol. Chem.* **2012**, *393*, 1067−1077.

(5) Ravishankara, A. R.; Daniel, J. S.; Portmann, R. W. Nitrous Oxide (N_2O): The Dominant Ozone-Depleting Substance Emitted in the 21st Century. *Science* **2009**, *326*, 123−125.

(6) Prasad, S. S. Potential New Atmospheric Sources and Sinks of Odd Nitrogen: Sources Involving the Excited O_2, and the $N_2O•O_3$ species. *Geophys. Res. Lett.* **1998**, *25*, 2173−2176.

(7) Okabe, H. *Photochemistry of Small Molecules*; Wiley: New York, 1978.

(8) Matsuoka, M.; Ju, W. S.; Takahashi, K.; Yamashita, H.; Anpo, M. Photocatalytic Decomposition of N_2O into N_2 and O_2 at 298 K on Cu(I) Ion Catalysts Anchored onto Various Oxides. The Effect of the

Coordination State of the Cu(I) Ions on PHotocatalytic Reactivity. *J. Phys. Chem. B* **2000**, *104*, 4911−4915.

(9) Tolman, W. B. Binding and Activation of N_2O at Transition-Metal Centers: Recent Mechanistic Insights. *Angew. Chem., Int. Ed.* **2010**, *49*, 1018−1024.

(10) Severin, K. Synthetic Chemistry With Nitrous Oxide. *Chem. Soc. Rev.* **2015**, *44*, 6375−6386.

(11) Vaughan, G. A.; Sofield, C. D.; Hillhouse, G. L.; Rheingold, A. L. Oxygen-Atom Transfer from Nitrous Oxide. Identification of Intermediates in the Oxidation of Diphenylacetylene at Group 4 Metal Centers and the Structural Characterization of $(\eta\text{-}C_5Me_5)_2Ti\text{-}\{N(O)NCPh = CPh\}\cdot 1/2C_7H_8$. *J. Am. Chem. Soc.* **1989**, *111*, 5491−5493.

(12) Vaughan, G. A.; Hillhouse, G. L.; Rheingold, A. L. Syntheses, Structures, and Reactivities of Unusual Four-Membered Metallacycles Formed in Insertion Reactions of N = N=O, N = N=NR, and N = N=CR2 with $(\eta\text{-}C_5Me_5)_2Zr(C_2Ph_2)$. *J. Am. Chem. Soc.* **1990**, *112*, 7994−8001.

(13) Whited, M. T.; Grubbs, R. H. A Catalytic Cycle for Oxidation of Tert-Butyl Methyl Ether by a Double C-H Activation-Group Transfer Process. *J. Am. Chem. Soc.* **2008**, *130*, 16476−16477.

(14) Bottomley, F.; Brintzinger, H. H. Reactions of Nitrogen Oxides with Di(cyclopentadienyl)Titanium Complexes. *J. Chem. Soc., Chem. Commun.* **1978**, 234−235.

(15) Bottomley, F.; Lin, I. J. B.; Mukaida, M. Reactions of Dinitrogen Oxide (Nitrous Oxide) with Dicyclopentadienyltitanium Complexes Including a Reaction in Which Carbon Monoxide is Oxidized. *J. Am. Chem. Soc.* **1980**, *102*, 5238−5242.

(16) Vaughan, G. A.; Rupert, P. B.; Hillhouse, G. L. Selective O-atom Transfer from Nitrous Oxide to Hydride and Aryl Ligands of Bis(pentamethylcyclopentadienyl)hafnium Derivatives. *J. Am. Chem. Soc.* **1987**, *109*, 5538−5539.

(17) Harrold, N. D.; Waterman, R.; Hillhouse, G. L.; Cundari, T. R. Group-Transfer Reactions of Nickel-Carbene and -Nitrene Complexes with Organoazides and Nitrous Oxide that Form New C═N, C═O, and N═N Bonds. *J. Am. Chem. Soc.* **2009**, *131*, 12872−12873.

(18) Hutchings, G. J.; Comninos, H.; Copperthwaite, R. G.; van Rensburg, L. J.; Hunter, R.; Themistocleous, T. Reactivation of Zeolite and Oxide Catalysts Using Nitrous Oxide. *J. Chem. Soc., Faraday Trans. 1* **1989**, *85*, 633−644.

(19) Heyden, A.; Peters, B.; Bell, A. T.; Keil, F. J. Comprehensive DFT Study of Nitrous Oxide Decomposition over Fe-ZSM-5. *J. Phys. Chem. B* **2005**, *109*, 1857−1873.

(20) Armor, J. N.; Taube, H. Formation and reactions of $[(NH_3)_5RuN_2O^{2+}]$. *J. Am. Chem. Soc.* **1969**, *91*, 6874−6876.

(21) Paulat, F.; Kuschel, T.; Näther, C.; Praneeth, V. K. K.; Sander, O.; Lehnert, N. Spectroscopic Properties and Electronic Structure of Pentammineruthenium(II) Dinitrogen Oxide and Corresponding Nitrosyl Complexes: Binding Mode of N_2O and Reactivity. *Inorg. Chem.* **2004**, *43*, 6979−6994.

(22) Tuan, D. F. T.; Hoffmann, R. Nitrogen Atom vs. Oxygen Atom Linkage and Sigma.vs. Pi Bonding in Transition-Metal Complexes of Dinitrogen Oxide and Cyanate. *Inorg. Chem.* **1985**, *24*, 871−876.

(23) Pamplin, C. B.; Ma, E. S. F.; Safari, N.; Rettig, S. J.; James, B. R. The Nitrous Oxide Complex, $RuCl_2(\eta^1\text{-}N_2O)(P\text{-}N)(PPh_3)$(P-N = [o-(*N,N*-Dimethylamino)phenyl]diphenylphosphine); Low Temperature Conversion of N_2O to N_2 and O_2. *J. Am. Chem. Soc.* **2001**, *123*, 8596−8597.

(24) Piro, N. A.; Lichterman, M. F.; Harman, W. H.; Chang, C. J. A Structurally Characterized Nitrous Oxide Complex of Vanadium. *J. Am. Chem. Soc.* **2011**, 133, 2108−2111.

(25) Zhuravlev, V.; Malinowski, P. J. A Stable Crystalline Copper(I)−N_2O Complex Stabilized as the Salt of a Weakly Coordinating Anion. *Angew. Chem., Int. Ed.* **2018**, *57*, 11697−11700.

(26) Pomowski, A.; Zumft, W. G.; Kroneck, P. M. H.; Einsle, O. N_2O Binding at a [4Cu:2S] Copper−Sulphur Cluster in Nitrous Oxide Reductase. *Nature* **2011**, *477*, 234−237.

(27) Solomon, E. I.; Heppner, D. E.; Johnston, E. M.; Ginsbach, J. W.; Cirera, J.; Qayyum, M.; Kieber-Emmons, M. T.; Kjaergaard, C. H.; Hadt, R. G.; Tian, L. Copper Active Sites in Biology. *Chem. Rev.* **2014**, *114*, 3659−3853.

(28) Labios, L. A.; Millard, M. D.; Rheingold, A. L.; Figueroa, J. S. Bond Activation, Substrate Addition and Catalysis by an Isolable Two-Coordinate Pd(0) Bis-Isocyanide Monomer. *J. Am. Chem. Soc.* **2009**, *131*, 11318−11319.

(29) Carpenter, A. E.; Margulieux, G. W.; Millard, M. D.; Moore, C. E.; Weidemann, N.; Rheingold, A. L.; Figueroa, J. S. Zwitterionic Stabilization of a Reactive Cobalt Tris-Isocyandie Monoanion by Cation Coordination. *Angew. Chem., Int. Ed.* **2012**, *51*, 9412−9416.

(30) Barnett, B. R.; Moore, C. E.; Rheingold, A. L.; Figueroa, J. S. Cooperative Transition Metal/Lewis Acid Bond−Activation Reaction by a Bidentate (Boryl)iminomethane Complex: A Significant Metal−Borane Interaction Promoted by a Small Bite−Angle LZ Chelate. *J. Am. Chem. Soc.* **2014**, *136*, 10262−10265.

(31) Agnew, D. W.; Moore, C. E.; Rheingold, A. L.; Figueroa, J. S. Kinetic Destabilization of Metal−Metal Singel Bonds: Isolation of a Pentacoordinate Manganese(0) Monoradical. *Angew. Chem., Int. Ed.* **2015**, *54*, 12673−12677.

(32) Barnett, B. R.; Labios, L. A.; Moore, C. E.; England, J.; Rheingold, A. L.; Wieghardt, K.; Figueroa, J. S. Solution Dynamics of Redox Noninocent Nitrosoarene Ligands: Mapping the Electronic Criteria for the Formation of Persistent Metal−Coordinated Nitroxide Radicals. *Inorg. Chem.* **2015**, *54*, 7110−7121.

(33) Martin, G. J.; Martin, M. L.; Gouesnard, J. P. *^{15}N−NMR Spectroscopy*; Springer: Berlin, 1981.

(34) It has been previously reported for frustrated Lewis pairs (FLPs) that N_2O activation, resulting in a significant bending of the N−N−O angle, generates J_{NN} ^{15}N NMR coupling constants that are larger than those found in free N_2O: Neu, R. C.; Otten, E.; Lough, A.; Stephan, D. W. The Synthesis and Exchange Chemistry of Frustrated Lewis Pair−Nitrous Oxide Complexes. *Chem. Sci.* **2011**, *2*, 170−176.

(35) Werner, H.; Leonhard, K.; Burschka, C. Basische Metalle: IX Synthesen und Kristallstruktur von $C_5H_5Co(PMe_3)CS_2$. Reaktionen zu Zweikernkomplexen mit Co(SCS)Cr- und Co(SCS)Mn- Brückenbindungen. *J. Organomet. Chem.* **1978**, *160*, 291−298.

(36) Brookhart, M.; Lincoln, D. M.; Volpe, A. F.; Schmidt, G. F. Ligand Substituent Effects on the Dynamics and Structure of Agostic Ethylenecobalt Complexes of the Type $C_5R_5(L)Co(CH_2CHR'\text{-}\mu\text{-}H) + BF_4^-$ [L = $P(OMe)_3$, PMe_3; R = H, Me; R' = H, Me]. *Organometallics* **1989**, *8*, 1212−1218.

(37) Butenschön, H.; Kettenbach, R. T.; Krüger, C. Inhibition of the [2 + 2+2] Cyclization by the Formation of Chelates: Alkyne and Vinylidene Complexes with Cyclopentadienylcobalt(I). *Angew. Chem., Int. Ed. Engl.* **1992**, *31*, 1066−1068.

(38) Foerstner, J.; Kakoschke, A.; Stellfeldt, D.; Butenschön, H.; Wartchow, R. Reactions of a Chelated Cyclopentadienylcobalt(I) Complex with 3,3-Disubstituted Cyclopropenes: Formation of Isoprene, Vinylcarbene, and 1−Phosphadiene Ligands at the Metal. *Organometallics* **1998**, *17*, 893−896.

(39) Baldridge, K. K.; Bunker, K. D.; Vélez, C. L.; Holland, R. L.; Rheingold, A. L.; Moore, C. E.; O'Connor, J. M. Structural Characterization of $(C_5H_5)Co(PPh_3)(\eta^2\text{-alkene})$ and $(C_5H_5)Co(\eta^2\text{-alkyne})$ Complexes of Highly Polarized Alkynes. *Organometallics* **2013**, *32*, 5473−5480.

(40) Thiel, I.; Spannenberg, A.; Hapke, M. Synthesis of Air-Stable and Recyclable $CpCo^I$-Complexes. *ChemCatChem* **2013**, *5*, 2865−2868.

(41) Döring, S.; Erker, G. Preparation of 1,2,3,4-Tetramethylpentafulvene by Hydride Anion Abstraction from Lithium Pentamethylcyclopentadienide Employing Tritylchloride. *Synthesis* **2001**, *2001*, 43−45.

DOI: 10.1021/jacs.9b08241
J. Am. Chem. Soc. 2019, 141, 15003−15007